

# DEVELOPMENT OF CARRIER-PHASE-BASED TWO-WAY SATELLITE TIME AND FREQUENCY TRANSFER (TWSTFT)

**Blair Fonville, Demetrios Matsakis**  
Time Service Department  
U.S. Naval Observatory  
Washington, DC 20392, USA

**Alexander Pawlitzki and Wolfgang Schaefer**  
TimeTech GmbH  
D-70569 Stuttgart, Germany

## Abstract

*For the dissemination of precise time and frequency, the use of the Two-Way Satellite Time and Frequency Transfer (TWSTFT) method has, in recent years, become increasingly valuable. By the application of spread-spectrum technology, a client station, located anywhere within a common satellite's footprint, can link to a reference station and compare or synchronize its clock to the reference clock within nanoseconds or better with high levels of confidence. But as the frequency stabilities of today's sophisticated atomic-level clocks improve, so must the stability of a Two-Way system's method of time and frequency transfer. Carrier-phase information holds the promise of improving the stabilities of TWSTFT measurements, because of the great precision at which frequency transfers can be achieved. The technique requires that each site observe both its own satellite-translated signal and that of the cooperating site. As was reported in earlier papers, the translation frequency of the satellite itself is an additional unknown factor in the measurement, and it must be taken into consideration. However, it can be shown that simple estimates of the satellite's local oscillator (LO) frequency will suffice. Recent work has been conducted with implementation of the signal carrier-phase in operational TWSTFT links. The purpose of this paper is to discuss this recent work, with emphasis on the system's development.*

## I. INTRODUCTION

At the present state of the art, one of the primary tools for the dissemination of precise time and frequency is a Two-Way Satellite Time and Frequency Transfer (TWSTFT) system. With such a system, a client station and a reference station each employ a code division multiple access (CDMA) scheme to lock onto each other and establish communication. The spreading function used for the CDMA, while providing the spread-spectrum capability and all of the associated benefits, also provides time markers from each station's respective timescale. This allows the client station to synchronize its time to that of the linked reference station. Such a system is illustrated below in Figure 1 [1].

# Report Documentation Page

*Form Approved  
OMB No. 0704-0188*

Public reporting burden for the collection of information is estimated to average 1 hour per response, including the time for reviewing instructions, searching existing data sources, gathering and maintaining the data needed, and completing and reviewing the collection of information. Send comments regarding this burden estimate or any other aspect of this collection of information, including suggestions for reducing this burden, to Washington Headquarters Services, Directorate for Information Operations and Reports, 1215 Jefferson Davis Highway, Suite 1204, Arlington VA 22202-4302. Respondents should be aware that notwithstanding any other provision of law, no person shall be subject to a penalty for failing to comply with a collection of information if it does not display a currently valid OMB control number.

1. REPORT DATE <b>2005</b>	2. REPORT TYPE <b>N/A</b>	3. DATES COVERED <b>-</b>	
4. TITLE AND SUBTITLE <b>Development of Carrier-Phase-Based Two-Way Satellite Time and Frequency Transfer (TWSTFT)</b>		5a. CONTRACT NUMBER	
		5b. GRANT NUMBER	
		5c. PROGRAM ELEMENT NUMBER	
6. AUTHOR(S)		5d. PROJECT NUMBER	
		5e. TASK NUMBER	
		5f. WORK UNIT NUMBER	
7. PERFORMING ORGANIZATION NAME(S) AND ADDRESS(ES) <b>US Naval Observatory 3450 Massachusetts Ave, NW Washington, DC 20392</b>		8. PERFORMING ORGANIZATION REPORT NUMBER	
9. SPONSORING/MONITORING AGENCY NAME(S) AND ADDRESS(ES)		10. SPONSOR/MONITOR'S ACRONYM(S)	
		11. SPONSOR/MONITOR'S REPORT NUMBER(S)	
12. DISTRIBUTION/AVAILABILITY STATEMENT <b>Approved for public release, distribution unlimited</b>			
13. SUPPLEMENTARY NOTES <b>The original document contains color images.</b>			
14. ABSTRACT			
15. SUBJECT TERMS			
16. SECURITY CLASSIFICATION OF:			17. LIMITATION OF ABSTRACT
a. REPORT <b>unclassified</b>	b. ABSTRACT <b>unclassified</b>	c. THIS PAGE <b>unclassified</b>	<b>UU</b>
			18. NUMBER OF PAGES <b>16</b>
			19a. NAME OF RESPONSIBLE PERSON

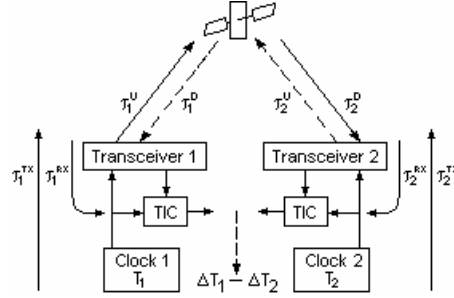


Figure 1. A basic Two-Way system.

A CDMA-based TWSTFT system measures the time difference between two clocks, and can provide frequency by differentiating the time-difference measurements. However, the CDMA-based TWSTFT method utilizes the carrier wave of the signal and not the superimposed lower-frequency pseudorandom noise (PRN) code. Therefore, CDMA-based TWSTFT suffers more from multipath effects, which is a function of effective wavelength, than does the carrier signal. Additionally, it is only the change of the relative phase that matters; an initial phase offset induced by multipath and the ionosphere has no relevance. For the same reason, other time delays introduced into the system, such as Sagnac effects and uncalibrated static time delays within user equipment, will have less effect on a carrier-phase system than in the code-based TWSTFT configuration.

Previous efforts to use the carrier-phase in TWSTFT have developed the system’s fundamental equations, and the results have shown some promise [2]. In this paper, we discuss the derivation of the system’s fundamental equations, followed by the results of two test runs: a collocated test at USNO, and an intercontinental test between PTB and USNO.

## II. CREATION OF THE SOLUTION EQUATION SET

In general, the carrier frequency of a received signal will be offset from the frequency generated by the transmitter. The magnitude of the frequency offset can be mostly attributed to four system-variables (illustrated below in Figure 2):  $f_{sLO}$ ,  $k_1$ ,  $k_2$ , and  $df$  [2], which are defined in the discussion to follow.

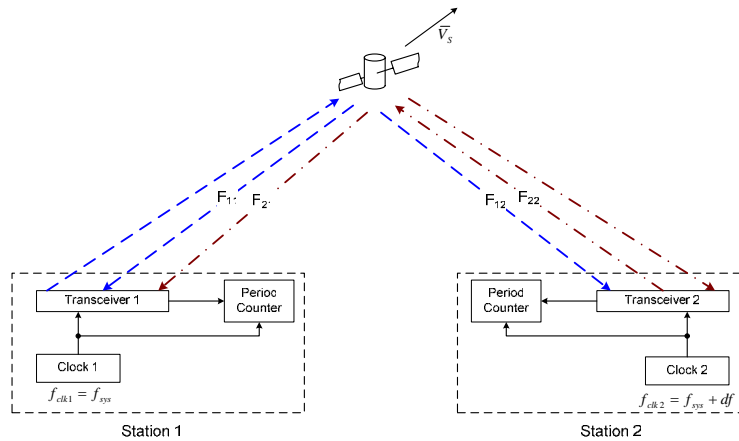


Figure 2. Carrier-Phase Two-Way.

As shown in the above figure, the reference station's (Station 1) time is based on a frequency  $f_{sys}$  and the frequency of Clock 2 is offset from  $f_{sys}$  by a value  $df$ . Realization of the offset between the frequencies of Clock 1 and Clock 2 is the basis of this paper.

A simple comparison of the transferred signals will not yield a true value of  $df$  due to three frequency perturbations (or frequency shifts) to which the carriers are subjected: two caused by the motion of the satellite and one caused by the satellite's unknown local oscillator frequency, or  $f_{SLO}$ . As an example, consider a one-sided carrier-frequency transfer depicted in Figure 2, where Station 1 is transmitting a signal to Station 2. The signal, which is relayed to Station 2 by a satellite, is subject to the Doppler effects resulting from the slight motion of the satellite. The first-order Doppler coefficients are described by the following two equations.

$$k_1 = \frac{\bar{V}_1}{c} \quad (1)$$

$$k_2 = \frac{\bar{V}_2}{c} \quad (2)$$

where  $\bar{V}_n$  is a projection of the velocity vector of the satellite in the direction of Station  $n$  and  $c$  is the speed of light through the transmission medium. Note that in Figure 2, the velocity of the satellite has been represented as a vector  $\bar{V}_s$ . Suppose that Station 1 transmits a signal with a frequency  $f_{tx}$ , where  $f_{tx}$  is defined with respect to (w.r.t.) the system frequency  $f_{sys}$ . At the satellite, the frequency of the received signal is centered at the Doppler-shifted frequency  $f_{tx} + k_1 f_{tx}$ , which is then mixed with the satellite's local oscillator (LO) and retransmitted at the carrier frequency given by the following equation:

$$f_{SV} = f_{tx} + k_1 f_{tx} - f_{SLO} \quad (3)$$

The carrier frequency is then observed Doppler-shifted at the downlink site as:

$$f_d = (f_{tx} + k_1 f_{tx} - f_{SLO}) + k_2 (f_{tx} + k_1 f_{tx} - f_{SLO}) \quad (4)$$

All of the frequencies given in Equation (4) are referenced to the system frequency. However, the value of  $f_d$  will be measured with reference to the receiver's local clock. Equation (4) must, therefore, be rewritten such that its terms are expressed with reference to the clock local to Station 2.

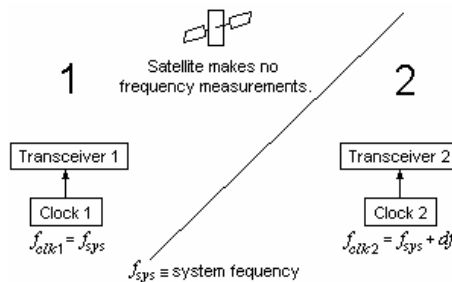


Figure 3. System frames of reference.

For the purpose of converting a given frequency, as defined by a frame of reference  $m$ , to its equivalent frequency, in a frame of reference  $n$ , a transformation equation has been derived:

$$f_n = f^m \left( \frac{fref^m}{fref_n} \right). \quad (5)$$

where  $f^m$  is the value of the frequency (w.r.t. the transmitter's clock), which is to be transformed;  $f_n$  is the value to be determined;  $fref^m$  is the instantaneous frequency of the reference clock at the transmitter (given w.r.t. system time); and  $fref_n$  is the instantaneous frequency of the reference clock at the receiver (given w.r.t. system time). Applying this transformation equation to the frequency transfer given by Equation (4) produces

$$F_{12} = f_{tx} \left( \frac{f_{sys}}{f_{sys} + df} \right) (1 + k_1)(1 + k_2) - f_{SLO} \left( \frac{f_{sys}}{f_{sys} + df} \right) (1 + k_2) \quad (6)$$

where the notation  $F_{mn}$  is used to denote a frequency that has been transmitted by Station  $m$  and measured by Station  $n$ . Similarly, we may derive the frequency transfer from Station 2 to Station 1 as follows:

$$F_{21} = f_{tx} \left( \frac{f_{sys} + df}{f_{sys}} \right) (1 + k_1)(1 + k_2) - f_{SLO} (1 + k_1). \quad (7)$$

In addition to the two transfers given by Equations (6) and (7), each station may receive its own signal. These are modeled by the following two loopback equations:

$$F_{11} = f_{tx} (1 + k_1)^2 - f_{SLO} (1 + k_1) \quad (8)$$

$$F_{22} = f_{tx} (1 + k_2)^2 - f_{SLO} \left( \frac{f_{sys}}{f_{sys} + df} \right) (1 + k_2) \quad (9)$$

With theoretically ideal measurements, the values  $F_{11}$ ,  $F_{22}$ ,  $F_{12}$ , and  $F_{21}$  are independent; however, under the limitation of the system equipment's quantization noise, the following equality is satisfied:

$$F_{11} + F_{22} = F_{12} + F_{21} \quad (10)$$

This equality allows for an immediate data integrity check. Alternatively, it will be shown that it also allows the user to solve the system using only three of the four equations, thus sparing a receiver channel.

With the two carrier transfers and the two loopbacks defined above, the carrier-phase system is fully described and we now have four equations from which we may resolve our four system variables.

### III. UNDERSTANDING THE SYSTEM EQUATION SET

Generally speaking, the frequencies  $F_{11}$ ,  $F_{22}$ ,  $F_{12}$ , and  $F_{21}$  are provided by the two spread-spectrum modems employed by the system, and the frequencies are reported in the IF-band. Because the carrier-phase system is based on these measurements, it may be insightful to examine the construction of the values. Consider the following system, where the satellite is stationary with respect to both TWSTT stations:

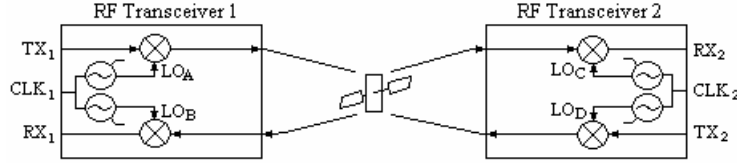


Figure 4. RF transceiver signal propagations.

Relating the above figure to the carrier-phase system, the illustrated signals have the following associated frequencies:

$$\begin{aligned}
 CLK_1 &\rightarrow f_{sys} \\
 CLK_2 &\rightarrow f_{sys} + df \\
 TX_1 &\rightarrow f_{tx} \\
 TX_2 &\rightarrow f_{tx} + y_0 f_{tx} \\
 LO_A &\rightarrow f_{LOtx} \\
 LO_B &\rightarrow f_{LOrx} \\
 LO_C &\rightarrow f_{LOrx} + y_0 f_{LOrx} \\
 LO_D &\rightarrow f_{LOtx} + y_0 f_{LOtx}
 \end{aligned}$$

where the instantaneous fractional frequency  $y_0$  is defined as

$$y_0 = \frac{df}{f_{sys}}. \quad (11)$$

As shown, the RF/IF mixers are supplied tunable synthesized frequencies from their respective LO's. It can be shown that the output frequencies of the synthesizers will have the same fractional frequencies as their inputs, with regard to  $f_{sys}$ . Now if the signal is traced from left to right (i.e. from the signal in the form of  $TX_1$  to form  $RX_2$ ), the following equation is obtained:

$$F_2 = f_{tx} + (f_{LOtx} - f_{LOrx}) - y_0 f_{LOrx} - f_{SLO}, \quad (12)$$

where  $F_2$  is the frequency of the signal denoted in the figure as  $RX_2$  and is given with respect to the system timescale. In general, the values  $f_{LOtx}$  and  $f_{LOrx}$  are tuned such that their difference models the nominal value of  $f_{SLO}$ . If we make the assumptions that the satellite's LO is ideal and that the tuning is perfect, Equation (12) becomes

$$F_2' = f_{tx} - y_0 f_{LOrx} \cdot \quad (13)$$

Using the transformation Equation (5), the transmitted frequency  $f_{tx}$  would be directly measured at the receiving end (with no up/down frequency translation or satellite relay) as

$$F_2'' = f_{tx} \left( \frac{f_{sys}}{f_{sys} + df} \right) = \frac{f_{tx}}{1 + y_0} \approx f_{tx} - y_0 f_{tx} \cdot \quad (14)$$

Since  $y_0 f_{LOrx} > y_0 f_{tx}$ , the observed frequency shift (13) is greater than the shift expected from the transformation (14) by a factor  $m_{nr}$ , which can be derived as follows:

$$\begin{aligned} f_{tx} - m_{nr} y_0 f_{tx} &= (f_{tx} - y_0 f_{LOrx}) \frac{f_{sys}}{f_{sys} + df} \quad (a) \\ \Rightarrow m_{nr} &= \frac{1}{y_0} - \frac{1}{y_0 + y_0^2} + \frac{1}{1 + y_0} \frac{f_{LOrx}}{f_{tx}} \quad (b) \\ \Rightarrow m_{nr} &= \frac{1}{1 + y_0} + \frac{1}{1 + y_0} \frac{f_{LOrx}}{f_{tx}} \quad (c) \\ \Rightarrow m_{nr} &= \left( \frac{f_{LOrx}}{f_{tx}} + 1 \right) * \frac{f_{sys}}{f_{sys} + df} \approx \frac{f_{LOrx}}{f_{tx}} + 1. \quad (d) \end{aligned} \quad (15)$$

Note that the right side of Equation (15a) is simply Equation (13) transformed through the use of the transformation Equation (5).

Similar to the derivation of Equation (12), proceeding from right to left produces

$$F_1 = f_{tx} + y_0 f_{tx} + (f_{LOtx} - f_{LOrx}) + y_0 f_{LOtx} - f_{SLO} \cdot \quad (16)$$

which, under the same assumptions as before, becomes

$$F_1' = f_{tx} + y_0 (f_{tx} + f_{LOtx}) \quad (17)$$

and it is seen that when the non-reference station is the transmitting station, the fractional frequency bias is multiplied by a factor of

$$m_r = \frac{f_{LOtx}}{f_{tx}} + 1 \quad (18)$$

where  $m_r$  is a coefficient of the clock's fractional frequency, as seen by the receiving reference station.

From the above discussion we see that, due to the fractional frequency multiplication effect of the Carrier-Phase Two-Way system, there is a reduction in the effective measurement quantization and, therefore, a reduction in the system's sensitivity to noise. As a concrete example, consider a receiving station *B* with a clock that is oscillating 1 mHz slower than the clock at a transmitting Station *A*, where both clocks have

nominal frequencies of 5 MHz. This equates to a fractional frequency deviation of  $-2 \times 10^{-10}$ . Suppose further that the receiving Station *B* is capable of making frequency measurements rounded to the nearest tenth of a hertz. Now, if both stations are collocated, no satellite communication is necessary and Station *B* can take a direct measurement of the Station *A* output. With an unlimited resolution and in the absence of measurement noise, Station *B* will record a value of 70,000,000.0140 Hz (assuming an IF nominal transmit frequency of 70 MHz). However, the actual value recorded is rounded to 70,000,000.0 Hz and the clocks are, therefore, erroneously determined to be in syntonization. Now consider a full Ku-band satellite transfer (as opposed to the collocated scenario) where the transmitter LO and the receiver LO are tuned to model a satellite turnaround frequency of 2 GHz, with the nominal values of 13.93 GHz and 11.93 GHz, respectively, to produce a 14/12 GHz transmit/receive pair when mixed with the 70 MHz IF. Using the coefficient derived in Equation (15), the fractional frequency of the received signal is multiplied from  $-2 \times 10^{-10}$  to approximately  $-3.43 \times 10^{-8}$  and the rounded measurement  $F_B$  is then equal to 70,000,002.4 Hz. From this value, the two Stations will deduce that their fractional frequency deviation is

$$y_0 = \frac{f_{tx} - F_B}{m_{nr} f_{tx}} = \frac{(70,000,000 - 70,000,002.4) \text{ Hz}}{171.43 * 70,000,000 \text{ MHz}} \approx -1.99998 \times 10^{-10}, \quad (19)$$

and the result is very close to the actual clock frequency deviation (i.e.  $-2 \times 10^{-10}$ ).

## IV. SOLVING THE SYSTEM

The four nonlinear system equations (Equations (6)-(9)) may be solved by several different numerical techniques. One method begins by linearizing the four equations about some initial estimation vector  $\tilde{x} = [\tilde{f}_{SLO}, \tilde{k}_1, \tilde{k}_2, \tilde{df}]$  as follows [3]:

$$\begin{bmatrix} \delta F_{11} \\ \delta F_{22} \\ \delta F_{12} \\ \delta F_{21} \end{bmatrix} = \begin{bmatrix} -(1+\tilde{k}_1) & -\tilde{f}_{SLO} + 2f_{tx}(1+\tilde{k}_1) & 0 & 0 \\ -f_{sys}(1+\tilde{k}_2) & 0 & -\frac{f_{sys}\tilde{f}_{SLO}}{f_{sys} + \tilde{df}} + 2f_{tx}(1+\tilde{k}_2) & \frac{f_{sys}\tilde{f}_{SLO}(1+\tilde{k}_2)}{(f_{sys} + \tilde{df})^2} \\ \frac{f_{sys} + \tilde{df}}{-f_{sys}(1+\tilde{k}_2)} & \frac{f_{sys}f_{tx}(1+\tilde{k}_2)}{f_{sys} + \tilde{df}} & -f_{sys}\frac{\tilde{f}_{SLO} - f_{tx}(1+\tilde{k}_1)}{f_{sys} + \tilde{df}} & (1+\tilde{k}_2)f_{sys}\frac{\tilde{f}_{SLO} - f_{tx}(1+\tilde{k}_1)}{(f_{sys} + \tilde{df})^2} \\ \frac{f_{sys} + \tilde{df}}{-f_{sys}(1+\tilde{k}_1)} & -\tilde{f}_{SLO} + f_{tx}(1+\tilde{k}_2)\frac{f_{sys} + \tilde{df}}{f_{sys}} & f_{tx}(1+\tilde{k}_1)\frac{f_{sys} + \tilde{df}}{f_{sys}} & f_{tx}(1+\tilde{k}_1)\frac{1+\tilde{k}_2}{f_{sys}} \end{bmatrix} \begin{bmatrix} \delta \tilde{f}_{SLO} \\ \delta \tilde{k}_1 \\ \delta \tilde{k}_2 \\ \delta \tilde{df} \end{bmatrix} \quad (20)$$

where

$$\delta F_i = F_i(f_{SLO}, k_1, k_2, df) - F_i(\tilde{f}_{SLO}, \tilde{k}_1, \tilde{k}_2, \tilde{df}). \quad (21)$$

For simplicity, Equation (20) is re-written as

$$\overline{\delta F} = G \overline{\delta x} \quad (22)$$

where *G* is generally referred to as the geometry matrix. The state estimate error-vector  $\overline{\delta x}$ , of the above equation, contains updates to the estimation vector  $\tilde{x}$  and summing the two improves the accuracy of the



values contained in  $\tilde{x}$ . This method, commonly known as the Newton-Raphson method, may then iterate while  $\overline{\delta x}$  converges to zero.

However, the determinant of matrix G is equal to 0 and the linearized system is, therefore, singular. As such, no unique solution exists and the matrix system given by Equation (22) is not directly solvable, but necessitates some additional numerical method, such as Singular Value Decomposition (SVD). However, it is known that the values  $k_1$ ,  $k_2$ , and  $df$  will be very close to 0, and it can be shown that the system is resistant to imperfect approximations of  $f_{SLO}$ . Therefore, if the estimation  $\tilde{k}_1 = \tilde{k}_2 = \tilde{df} = 0$  is made, and  $\tilde{f}_{SLO}$  is assumed to be known and constant at its nominal value, a single iteration will suffice and Equation (20) is forced to the static equation set

$$\begin{bmatrix} F_{11} - f_{tx} + f_{SLO} \\ F_{22} - f_{tx} + f_{SLO} \\ F_{12} - f_{tx} + f_{SLO} \\ F_{21} - f_{tx} + f_{SLO} \end{bmatrix} = \begin{bmatrix} -f_{SLO} + 2f_{tx} & 0 & 0 \\ 0 & -f_{SLO} + 2f_{tx} & \frac{f_{SLO}}{f_{sys}} \\ f_{tx} & -f_{SLO} + f_{tx} & \frac{f_{SLO} - f_{tx}}{f_{sys}} \\ -f_{SLO} + f_{tx} & f_{tx} & \frac{f_{tx}}{f_{sys}} \end{bmatrix} \begin{bmatrix} k_1 \\ k_2 \\ df \end{bmatrix}. \quad (23)$$

If Equation (23) is further reduced by treating  $k_1$  as an independent variable, the system may be generalized by the geometric figure illustrated below.

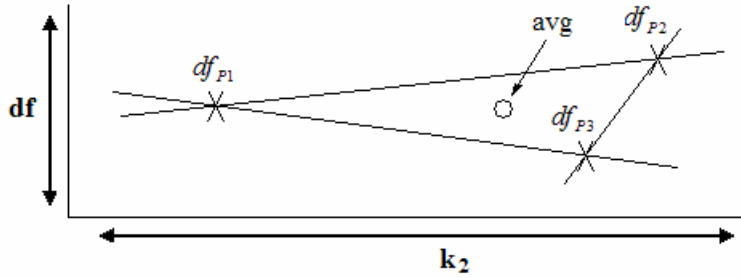


Figure 5. The three solution points and their average.

As shown in Figure 5, Equation (23) produces three lines with three different points of intersection:

$$\begin{aligned} df_{P1} &= f_{sys} \left( \frac{(f_{tx} - f_{SLO})(F_{11} - F_{22}) + (f_{SLO} - 2f_{tx})(F_{11} - F_{12})}{-2f_{tx}(f_{tx} - f_{SLO})} \right) \\ df_{P2} &= f_{sys} \left( \frac{(2f_{tx} - f_{SLO})(F_{11} - F_{21}) - f_{tx}(F_{11} - F_{22})}{-2f_{tx}(f_{tx} - f_{SLO})} \right) \\ df_{P3} &= f_{sys} \left( \frac{f_{tx}(F_{21} - F_{12}) + f_{SLO}(F_{11} - F_{21})}{2f_{tx}(f_{tx} - f_{SLO})} \right) \end{aligned} \quad (24)$$

where, if the equality of Equation (10) holds, each of these three solution points is expected to be equal. This allows the user the option to use just one equation, involving any three of the  $F_{mn}$ , thus sparing a

receiver channel for unrelated business. Alternatively, to minimize the effect of noise, the three points may be averaged as

$$df_{AVG} = \frac{f_{sys}}{6} \left( \frac{f_{SLO}(F_{12} - F_{22}) + 2f_{SLO}(F_{11} - F_{21}) - 3f_{ix}(F_{12} - F_{21})}{f_{ix}(f_{ix} - f_{SLO})} \right). \quad (25)$$

If all four channels are used, an integrity check can be made based on the consistency of the three solutions in Equations (24).

## V. RESIDUAL ERRORS

Our previous assumption that  $f_{SLO}$  is static and nominal will cause our resultant approximate solution to deviate from its ideal position. Likewise, inaccuracies of the linearizations (i.e. truncation of the high-order terms from the Taylor Series expansions) will cause errors in the solution. Other sources of error include (but are not limited to) troposphere dynamics, ionosphere dynamics, system noise, measurement noise, and multipath. An attempt to approximate the effects of some of these error sources is provided below in Table 1 [4,5].

Source	Magnitude	Resulting Error (ff)*
Modem quantization	$\frac{1 \text{ MHz}}{70 \text{ MHz}} \approx 1.43 \times 10^{-11}$	$\sim 2 \times 10^{-13} / \text{tau}$
Linearization	$k = 6.7 \times 10^{-9}$ $f_{SLO} = 1 \times 10^{-7}$ $df_{\text{clocks}} = 1 \times 10^{-11}$	$< 1 \times 10^{-16}$
Unmodeled zenith troposphere	500 ps/day	$\sim 2.6 \times 10^{-15}$
IGS troposphere maps	10 ps/hr RMS	$\sim 1.3 \times 10^{-15}$
Unmodeled zenith ionosphere**	50 TECU / 12 hrs	$\sim 5 \times 10^{-15}$
IGS ionosphere maps**	3 TECU / 2 hrs	$\sim 3 \times 10^{-15}$
Locally measured sinusoid model**	2 TECU / 24 hrs	$< 1 \times 10^{-16}$

\* Computed for Ku-band uplink and downlink frequencies of 12 and 14 GHz

\*\* At GPS frequencies, 2 TECU causes a delay of roughly 1 ns

Table 1. Sensitivity of derived frequency transfer to modeling errors.

These error sources are non-Gaussian. The magnitudes used in the table depict “worst-case,” but observable, variations. For  $\text{tau} < 100$  seconds, the dominating error is the 1 MHz quantization of the TWSTFT modems, which currently provides 1 MHz resolution at IF. Future modem revisions are expected to improve this figure.

## VI. RESULTS

Two preliminary tests have been prepared for inclusion in this report; the results of these test runs make it clear that, while the theoretical aspects of the system are sound, more work is required before carrier-phase TWSTFT can become fully operational.

The first test case was conducted using two collocated stations at USNO. The 86,400 fractional frequency data points, shown in Figure 6 (below), was calculated with the  $df_{p3}$  result of Equation (24). The data show a modulating frequency with a rate of approximately 0.8 mHz, or about 21 minutes (see Figures 7 and 8), and this is reflected in the Allan deviation plot shown in Figure 9. Subsequent tests have suggested that the problem may be traced to low-level frequency generations within the spread-spectrum modems. Specifically, if a frequency which is to be generated within a modem's direct digital synthesis (DDS) block is not an exact multiple of the DDS's minimum incremental resolution, it is compensated for by the phase-lock loop and an artificial frequency modulation can occur at the PLL output. However, it is also possible that the witnessed data variations are simply due to temperature fluctuations or other environmental effects. These possibilities are currently under investigation.

Figure 10 shows the Allan deviation from a day of carrier-phase TWSTFT sessions involving stations at both USNO and Physikalisch Technische Bundesanstalt (PTB). While we were unable to produce enough uninterrupted data to provide stability calculations beyond 4000 seconds, it is evident that there exist oscillations within these data as well. It is interesting to note, that the oscillations in this data set are at a higher rate than the 0.8 mHz frequency seen in the collocated data.

## VII. CONCLUSION

In this paper, we have refined previously published techniques for calculating the carrier-phase two-way solution. The paper suggests a method of solving the system and then presents a simple error analysis. Worst-case error dependencies related to quantization, linearization, and atmospheric effects of ionosphere and troposphere are shown. We conclude that, with an ideal carrier-phase modem, a  $2 \times 10^{-15}$  frequency transfer at 1 second is possible.

Two-Way modems used at many of today's TAI laboratories have limitations due to the modems' current measurement resolution. Our bench tests and live experiments demonstrate these limitations. While it is unclear what is causing the additional noise, several possibilities, including frequency synthesis within the modems, are being explored. These unknown effects must be well understood before the carrier-phase TWSTFT system becomes fully operational, in order to maintain consistency and accuracy within the system's error budget.

## VIII. ACKNOWLEDGMENTS

The authors would like to thank Ed Powers, Angela McKinley, Alan Smith, and Paul Wheeler of USNO for their ongoing assistance with this project, and PTB for their contribution of the Two-Way data.

## IX. REFERENCES

- [1] D. Kirchner, 1991, “Two-Way Time Transfer Via Communication Satellites,” **Proceedings of the IEEE**, **79**, 983-990.
- [2] W. Schäfer, A. Pawlitzki, and T. Kuhn, 2000, “New Trends in Two-Way Time and Frequency Transfer via Satellite,” in Proceedings of the 31<sup>st</sup> Annual Precise Time and Time Interval (PTTI) Systems and Applications Meeting, 7-9 December 1999, Dana Point, California, USA (U.S. Naval Observatory, Washington, D.C.), pp. 505-514.
- [3] E. Kaplan, 1996, **Understanding GPS Principles and Applications** (Artech House Publishers, Norwood, Massachusetts), pp. 45-47.
- [4] P. Misra and P. Enge, 2001, **Global Positioning System: Signals, Measurements, and Performance** (Ganga-Jamuna Press, Lincoln, Massachusetts).
- [5] IGS Central Bureau, “IGS Products,” International GPS Service, 21 January 2005, <http://igs.cb.jpl.nasa.gov/components/prods.html>

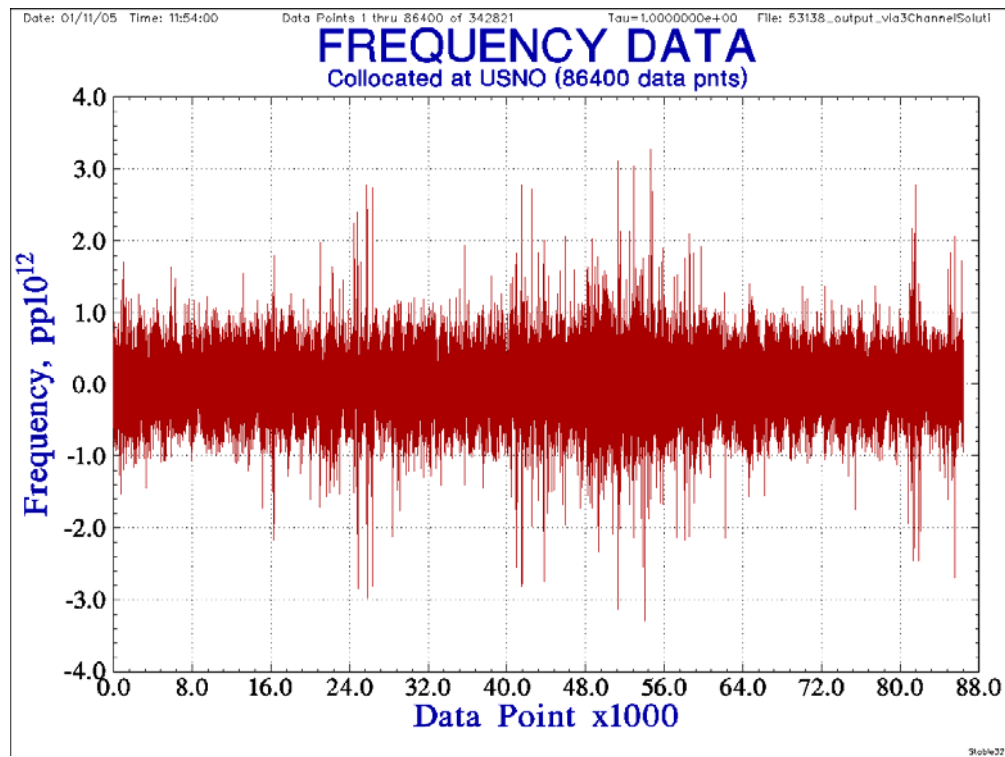


Figure 6. Fractional frequency collocated data (1-second data points) collected at USNO. Outliers that exceed a sigma factor of 10.0 were removed.

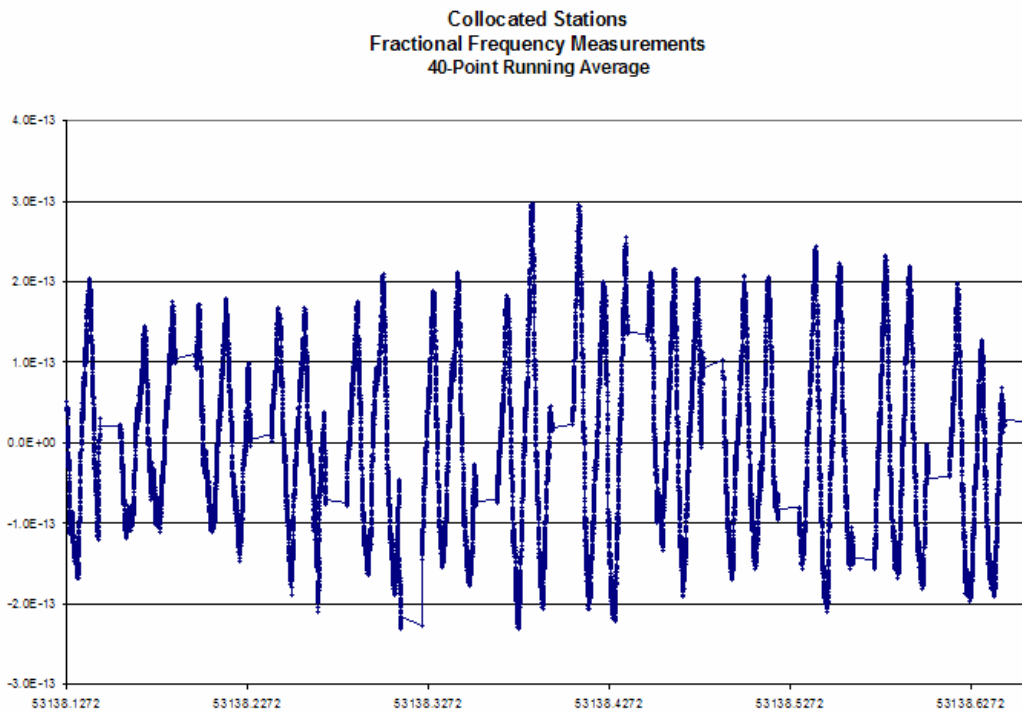


Figure 7. A 40-point running average of the collocated fractional frequency data accentuates the modulating 0.8 mHz frequency.

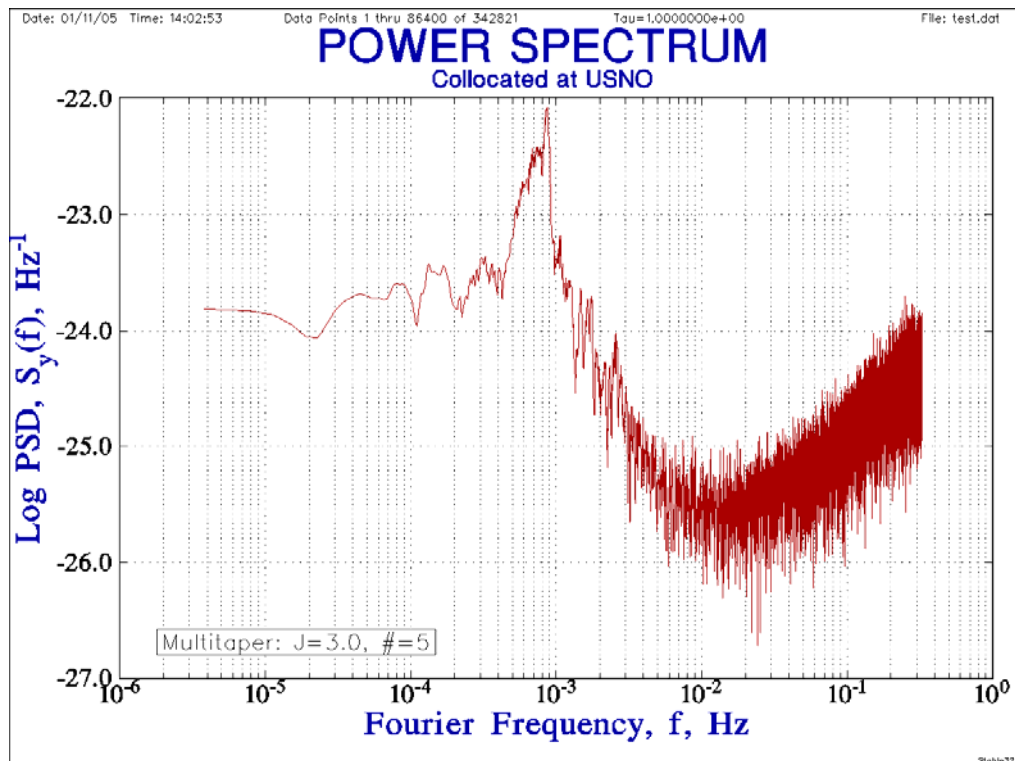


Figure 8. The power spectrum of the collocated fractional frequency data shows that the frequency of the modulating signal is approximately 0.8 mHz.

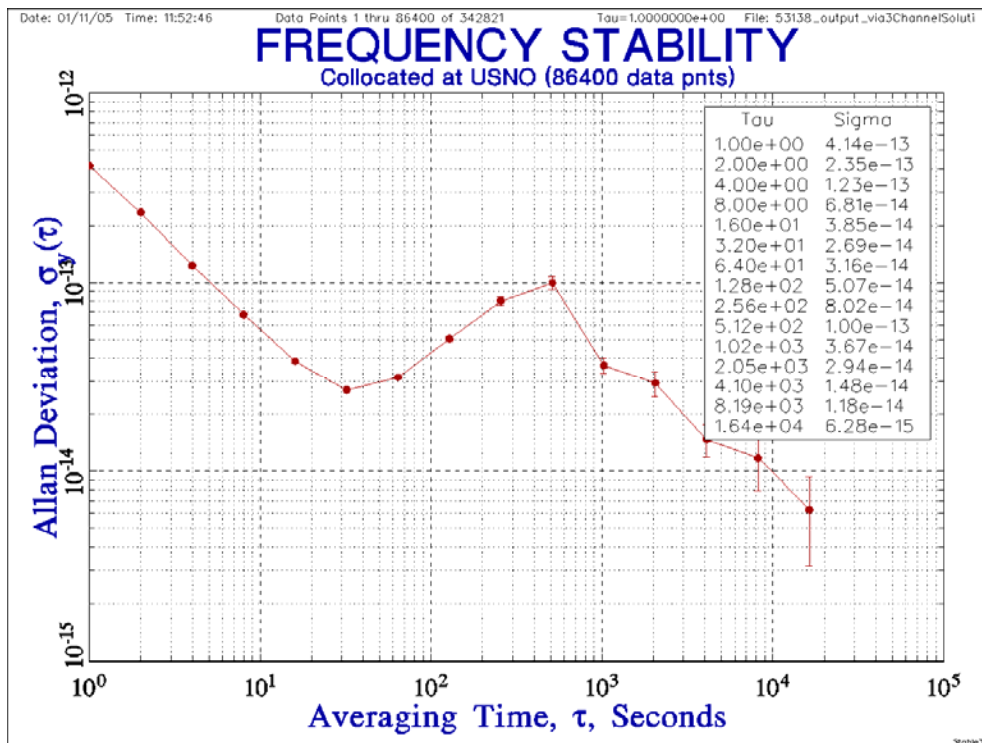


Figure 9. Allan Deviation plot of the collocated results (1-second data).

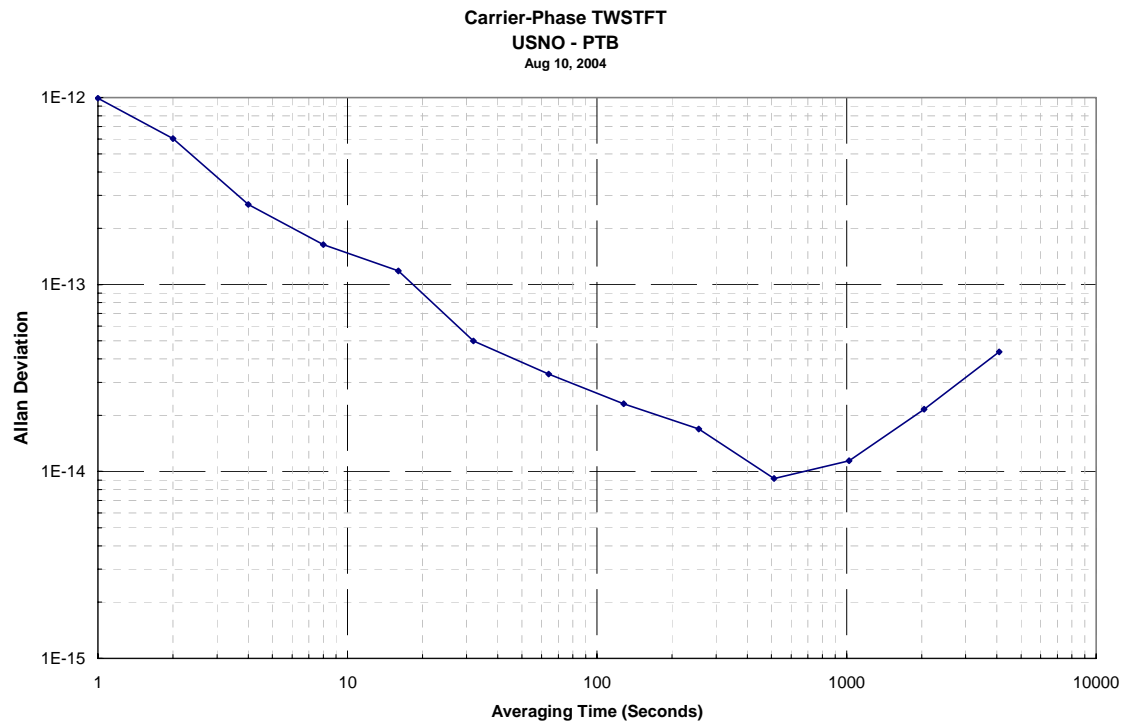


Figure 10. Carrier-Phase TWSTFT session between USNO and PTB.

## QUESTIONS AND ANSWERS

**TOM BAHDER (U.S. Army Research Laboratory):** When you set up the whole model, what reference frame – are you in a rotating, or are you in an ECI frame?

**BLAIR FONVILLE:** Well, the satellite is geostationary, so we set up each equation and derive all frequencies with respect to a system reference station.

**BAHDER:** But then you are implementing everything in a rotating frame, right? And my other question is then there must be some kind of a Sagnac effect that you should be seeing.

**FONVILLE:** Yes, we may see some slight drifts due to uncorrected Sagnac in the long term, but we haven't been able to take data over 15-minute spans. Like I say, diurnal effects are also something we need to investigate.

**BAHDER:** You could avoid the Sagnac term if you did the whole implementation in the ECI frame. But then you would have relative velocities of the ground stations and the satellites, and that would have to come into the problem.

**FONVILLE:** The relative velocities of the ground stations to the satellite is something we do account for. Thank you for that comment.

**CHRISTINE HACKMAN (University of Colorado):** You put up a viewgraph where you were talking about all the errors, and you showed two parts in  $10^{15}$  for the troposphere.

**FONVILLE:** Yes, I knew you were going to ask something about that – after your presentation.

**HACKMAN:** So are you assuming it is not going to cancel? Could you elaborate on that a little?

**FONVILLE:** The troposphere will not cancel because we are operating at two different sites.

**HACKMAN:** I guess what I normally understood in regular Two-Way, you are kind of going for this.

**FONVILLE:** Oh, I see. Yes, well, we have a transfer from one site to the other and vice versa, but we also have two loopbacks. And so those two loopbacks are where it does not cancel. We have a loopback on one side, we have a loopback on the other; they have different tropospheric paths, so it is not going to cancel there.

**WLODZIMIERZ LEWANDOWSKI (Bureau International des Poids et Mesures):** I have a short question. What is your feeling about the future of this approach? When can we expect the operation technique?

**FONVILLE:** That is a good question. This is all very preliminary, but the results are encouraging. So it does give us some motivation to continue the effort. It can be in operation relatively quickly. But it is contingent on how the longer periods look. For instance, we have had some data that – well, in the 15 minutes that I showed, it seems to be dropping without any problem. But we have concatenated contiguous sets of data, and tried to do some numerical calculations on it. And it seems to level off.



*36<sup>th</sup> Annual Precise Time and Time Interval (PTTI) Meeting*

So we may still have some processes that we have not yet fully investigated. So that is a difficult question to answer.